

Universitat de Lleida

Document downloaded from:

<http://hdl.handle.net/10459.1/71088>

The final publication is available at:

<https://doi.org/10.1016/j.cej.2016.11.081>

Copyright

cc-by-nc-nd, (c) Elsevier, 2016



Està subjecte a una llicència de
[Reconeixement-NoComercial-SenseObraDerivada 3.0 de Creative Commons](https://creativecommons.org/licenses/by-nc-nd/3.0/)

Accepted Manuscript

New polymeric/inorganic hybrid sorbents based on red mud and nanosized magnetite for large scale applications in As(V) removal.

Marta López-García, María Martínez-Cabanas, Teresa Vilariño, Pablo Lodeiro, Pilar Rodríguez-Barro, Roberto Herrero, José L. Barriada

PII: S1385-8947(16)31643-6
DOI: <http://dx.doi.org/10.1016/j.cej.2016.11.081>
Reference: CEJ 16082

To appear in: *Chemical Engineering Journal*

Received Date: 17 September 2016
Revised Date: 9 November 2016
Accepted Date: 10 November 2016

Please cite this article as: M. López-García, M. Martínez-Cabanas, T. Vilariño, P. Lodeiro, P. Rodríguez-Barro, R. Herrero, J.L. Barriada, New polymeric/inorganic hybrid sorbents based on red mud and nanosized magnetite for large scale applications in As(V) removal., *Chemical Engineering Journal* (2016), doi: <http://dx.doi.org/10.1016/j.cej.2016.11.081>

This is a PDF file of an unedited manuscript that has been accepted for publication. As a service to our customers we are providing this early version of the manuscript. The manuscript will undergo copyediting, typesetting, and review of the resulting proof before it is published in its final form. Please note that during the production process errors may be discovered which could affect the content, and all legal disclaimers that apply to the journal pertain.



New polymeric/inorganic hybrid sorbents based on red mud and nanosized magnetite for large scale applications in As(V) removal.

Marta López-García¹, María Martínez-Cabanas¹, Teresa Vilariño¹, Pablo Lodeiro², Pilar Rodríguez-Barro¹, Roberto Herrero¹ and José L. Barriada^{1*}

¹Universidade da Coruña, Departamento de Química Física e Enxeñaría Química I, Rúa da Fraga 10, 15071 A Coruña, Spain.

²GEOMAR, Helmholtz Ctr Oceans Res, D-24148 Kiel, Germany

*Corresponding author. Tel.: +34 881012261; fax: +34 981167065. e-mail address: jbarriada@udc.es (J.L. Barriada).

Abstract

Red mud (RM), a waste product generated in the industrial production of aluminium, was recovered for a second use as As(V) adsorbent. RM adsorption properties were compared to those obtained with a nanostructured in-lab synthesized iron oxide, magnetite. Operational problems associated with powdery consistency of raw materials were solved with the synthesis of new polymeric/inorganic hybrid sorbents by dispersing red mud and magnetite in chitosan. The behaviour of raw red mud and magnetite towards As(V) adsorption has been critically compared with that observed for the hybrid materials. pH dependence studies demonstrated that near neutral environments favour As(V) elimination. The sorption kinetics for the iron oxides showed that equilibrium was reached in less than 3 h for raw materials and up to 15 h for immobilized red mud and magnetite. The amount of arsenic sorbed on the four different sorbents as a function of the equilibrium arsenic concentration has been fitted to a Freundlich isotherm and a multilayer adsorption mechanism is proposed. Finally, continuous flow experiments were developed using chitosan immobilized red mud. Results allowed selecting batch conformation as the most effective for As(V) removal.

Keywords: Iron oxides; chitosan-hybrid material; sorption; arsenic.

1. Introduction

Arsenic is present in water as a result of both natural and anthropogenic activities. Inorganic arsenic can occur in the environment in several forms, in drinking water it is mostly found in trivalent (As(III)) or pentavalent (As(V)) oxidation states. Pollution in natural waters due to this metalloid is a worldwide problem and has been reported recently in the USA, China, Chile, Bangladesh, Taiwan, Mexico, Argentina, Poland, Canada, Hungary, New Zealand, Japan and India [1]. Arsenic dissolved in water is acutely toxic and can lead to a number of health problems. Arsenic is usually built up in the body through drinking water and food contaminated with arsenic and causes increased risks of cancer in the skin, lungs, liver, kidney, and bladder. To address the problem, the World Health Organization (WHO) guideline value and the European maximum permissible concentration (MPC) for arsenic in drinking water has been set as $10 \mu\text{g L}^{-1}$ [2, 3]. The US Environmental Protection Agency (USEPA) in 2001 also adopted a new standard for arsenic in drinking water at 10 ppb, replacing the old standard of 50 ppb [4]. A variety of arsenic-removal technologies are currently available including coprecipitation, adsorption in fixed-bed filters, anion exchange and reverse osmosis [1]; all of them are generally expensive. Arsenic removal in large-scale water treatment plants usually involves coagulation with Fe or Al salts. But processes based on adsorption and coprecipitation methods are promising because they can be used in small scale treatment plants, are easy to operate, may provide largely sludge-free operation, and may have a regeneration capability [5]. That is why an increasing attention is currently being paid to the development of new sorbents such as natural raw materials or agricultural and industrial wastes due to both their local abundance and low cost. Among the different available materials presenting arsenic sorption properties,

those containing metals, and especially iron, are known for being very effective sorbents. Iron (hydr)oxides are regarded as promising adsorbent materials as they have strong affinities towards inorganic arsenic species which result in high selectivity to arsenic in the sorption processes; moreover, they are low-cost and environmental friendly. Some examples of the different available materials presenting arsenic sorption are: iron hydroxide-coated alumina, manganese greensand and ferrihydrite [6] as well as iron based biomass-silica gel composites [7] or activated carbon loaded with iron [8].

However, fine powdery materials are not very appropriate for the treatment of industrial effluents using column systems, due to clogging effects. In addition, preconditioning is frequently required, using agglomeration procedures, to control hydrodynamic properties, at the expense of a significant loss in sorption efficiency [9]. This fact has motivated research in the use of different encapsulating agents, which allows improving raw material characteristics for large-scale application. An example of widely used immobilization agent is chitosan, a poly-N-glucosamine obtained by the de-acetylation of chitin, the second most abundant polysaccharide existing in the environment [10]. This biopolymer is highly hydrophilic and is characterized by a flexible polymer chain and by a large number of hydroxyl and amino groups that constitute potential adsorption sites. Moreover, it can be considered a low-cost material because it requires little processing, is abundant in nature and represents a by-product of fishery industry.

The capacity of chitosan for removing cations is well established, however much less is known and investigated about the ability of chitosan and chitosan derivatives to remove anionic forms of heavy metals [11]. Chitosan can be moulded in several shapes: membranes, microspheres, gel beads and films, and is able to provide a ratio surface area/mass that maximizes the adsorption capacity and minimizes the hydrodynamic limitation effects, such as column clogging and friction loss [12]. Besides chitosan,

other immobilization matrixes have also been studied, such as alginate to form beads incorporating the sorbent material, silicates to form soft gels where the sorbent can be dispersed, as well as polyurethane foams as supporting matrix of the active material [13].

Our research group has a wide experience in sorption studies of cationic metal pollutants using different types of biomass. However biomass has shown limited applicability for removing pollutants (metals or metalloids) as anionic species. Consequently our group has started the study of alternative sorbents for anionic pollutants. The present work deals with the adsorption properties of two iron oxide based materials, red mud (a Bayer process by-product) and in-lab synthesized magnetite nanoparticles. Magnetite was chosen as a model iron oxide with a well-defined structure and a high potential affinity for As(V) to compare its behaviour with the heterogeneous red mud powder, a cheap readily available industrial waste. Additionally, the magnetic properties of magnetite could be used for an easier way to remove this sorbent from solution. Moreover chitosan immobilization was also tested in order to improve raw adsorbents characteristics. Other immobilization matrixes were also tested, but showed worse to non-useful results. Raw materials were employed to select pH conditions for As(V) removal. Then, kinetic and equilibrium experiments were carried out to describe the adsorption process using both raw and immobilized adsorbents. Finally, batch results were compared with column experiments in order to select the best operational conformation for the application of chitosan coated red mud in the purification of arsenic polluted waters. The broad objective of this study is to present a new hybrid polymeric/inorganic sorbent with good adsorption features for As(V) removal, that does not need pretreatment such as pH adjustment and does not alter the water quality forming fine particulated suspensions.

2. Materials and methods

2.1. Materials

2.1.1. Chemicals

Reagents were used as supplied without further purification. FeSO_4 , NaBH_4 , alginic acid, CaCl_2 , chitosan, HCl , $\text{Na}_2\text{HAsO}_4 \cdot 7\text{H}_2\text{O}$ 98% PA were provided by Panreac (Panreac Química S.A., Barcelona, Spain), NaOH from Merck (Merck KGaA, Darmstadt, Germany) and sodium silicate purum from Sigma-Aldrich (Sigma-Aldrich Química, S.L). FOAM-iT!® 3 - 1A:1B kit (Smooth-on, Inc., Pennsylvania, US) was employed to obtain polyurethane foams. All solutions were prepared in deionized water.

2.1.2. Materials

Dry powdered red mud was obtained as a residue from an alumina production plant; this material was used without any pre-treatment. Nanoparticulated magnetite was synthesized following the procedure described by Yamaura and Alves [14]. Briefly, 500 μL of NaOH 2.5 M were added into a FeSO_4 solution in time intervals of 30 seconds until pH 11. After that, a black magnetic powder was observed in solution; this black mixture was then boiled in a water bath during 75 min. Afterwards, a strong magnet was used to retain the magnetite. The solid obtained was washed with deionized water until neutralization and dried in a vacuum desiccator. Magnetite characterization was performed on powdered samples in a Siemens Smart CCD 1k diffractometer. Magnetite was also characterized by Scanning Electron Microscopy (SEM) and Transmission Electron Microscopy (TEM). Studies were done with a JEOL JSM 6400 and a JEOL JEM 1010 (Jeol GmbH, München, Germany) respectively.

Hybrid materials were prepared from raw red mud and magnetite. Alginate based materials were prepared using 25 mL of 2% alginic acid solution where 0.3 g of raw

material was mixed up. Once homogenized, the mixture was added into a 50 mM CaCl_2 solution dropwise, obtaining alginate based beads. For chitosan based beads, 0.3 g of chitosan were dissolved in 25 mL of a 2% acetic acid solution. Then 0.3 g of raw material was added to the solution. Suspension was dripped into a 2 M NaOH solution, maintaining agitation during 12 h. Chitosan and alginate beads (diameter 2-3 mm) were washed with ultrapure water until neutralization and stored in ultrapure water in polyethylene bottles. Percentage of raw materials in the beads was close to 18%. The synthesis of silica based materials was carried out by a sol-gel process [15] 0.1 g of the chosen sorbent material was mixed with 2 mL of H_2O . Then 2 mL of 0.8 M Na_2SiO_3 solution was added and the mixture was stirred at 170 rpm (ELMI Sky line Shaker DOS-20M) to obtain a good dispersion of the material in the aqueous solution. After that, the required amount of 4 M HCl solution was added to achieve neutral pH. The mixture was continuously stirred until gel formation. Gels were refrigerated for at least 48 h and finally they were oven-dried during 2 h at 60°C. Polyurethane foams were prepared adding 0.3 g of raw material to the preparation mixture following the supplier specifications for FOAM-iT!® 3 - 1A:1B kit. Polyurethane foams were cut up in small cubes (≈ 0.5 cm) and stored in polyethylene flasks.

A stock solution of As (V) 1000 mg L^{-1} was prepared by dissolving the appropriate amount of $\text{Na}_2\text{HAsO}_4 \cdot 7\text{H}_2\text{O}$ in ultrapure water. As(V) solutions used in kinetic, adsorption and continuous flow experiments were prepared by diluting this stock solution with ultrapure water in order to obtain the desired As(V) concentrations.

2.2. Effect of solution pH

pH effect on arsenic adsorption was tested only for raw materials putting in contact 0.05 g of raw red mud or magnetite with 20 mL of 50 $\mu\text{g L}^{-1}$ As(V) solutions. pH was

adjusted using HCl or NaOH solutions as required. The experiments were developed at room temperature with rotary agitation during 3 h. After that, an aliquot of the supernatant solution was taken and centrifuged in a Nahita 2716 centrifuge (Auxilab, S.L., Navarra, Spain) for 3 min at 10000 rpm in order to separate the fine powder suspension. Total As concentration was determined by atomic adsorption spectrometry (Varian Spectra AA 55B Atomic Absorption Spectrometer). Hydride generation (HG-AAS) was used for low As(V) determination ($1\text{-}10\text{ }\mu\text{g L}^{-1}$) [16] using NaBH_4 , HCl and NaOH as reagents. Limit of detection (LOD) for As(V) was below $1\text{ }\mu\text{g L}^{-1}$.

2.3. Matrix selection

Several matrices, namely alginate, chitosan, silica and polyurethane foam were tested in order to select the best material for maximum As(V) removal. Batch experiments were carried out putting in contact 0.05 g of raw or hybrid materials with 20 mL of $50\text{ }\mu\text{g L}^{-1}$ As(V) in a conical flask. Mixtures were stirred on a rotary shaker (Compact Shaker KS-15, Edmund Bühler GmbH, Hechingen, Germany) at 175 rpm during 3 h (raw materials) or 24 h (hybrid materials) at room temperature. Studies were carried out at natural pH (≈ 7), except for red mud experiments, where natural pH was very high (≈ 10), therefore the solution pH was adjusted to 6.5-7 by addition of small volumes of a concentrated HCl solution. Aliquots of the supernatant solution were taken and analysed as mentioned above.

2.4. Kinetic studies

Equilibrium times were estimated using raw and hybrid chitosan materials. For this purpose 0.5 g of each raw material were put in contact with 200 mL of 1 mg L^{-1} As(V) solution in a thermostated vessel at 25°C . Red mud experiments were developed at pH 7 while in magnetite studies pH was not adjusted (natural pH=5).

For hybrid chitosan materials, kinetic experiments were developed following the same procedure used for raw adsorbents with the only difference of the material dose employed. For hybrid materials, the dose was higher than the one used with raw materials, in order to maintain the same raw adsorbent amount. Consequently, raw adsorbent percentage was determined for each wet hybrid adsorbent set. Using this value, wet beads were weighted to obtain 2.5 g L^{-1} of raw magnetite or red mud in each experiment. This allows comparing the results obtained with raw and hybrid materials on a raw material basis.

As(V) was determined by Flame atomic absorption spectrometry (FAAS); aliquots of each solution were taken at different times and centrifuged. Centrifuging was only required for batch experiments using raw materials, being very fine powders. Chitosan beads experiments did not require centrifugation of the already clear solution.

2.5. Equilibrium studies

The effect of initial concentration on adsorption capacities was studied putting in contact raw and hybrid chitosan materials with As(V) solutions in concentrations ranging between 1 and 1000 mg L^{-1} . Raw adsorbent dose was maintained at 2.5 g L^{-1} , as mentioned in the kinetic experiments section. Experiments were developed at room temperature; contact time was 3 h for raw materials and 24 h when hybrid materials were used. Once equilibrium was attained, aliquots were taken, centrifuged and As(V) concentration was determined using HG-AAS for low As(V) concentrations while FAAS was used for As(V) concentrations ranging from 3 to 30 mg L^{-1} . Centrifugation step was not necessary with hybrid materials.

Adsorption capacities were represented by q , the amount of As(V) adsorbed per gram of adsorbent, calculated as follows from a mass balance:

$$q = \frac{(C_i - C_f) \cdot V}{m} \quad (1)$$

where C_i and C_f are the initial and final As(V) concentrations in mg L^{-1} , V is the volume of solution in each experiment in L and m is the mass of adsorbate in g.

2.6. Column experiments

Continuous flow experiments were developed using a 3 cm internal diameter and 40 cm length column, filled with 20 g of chitosan coated red mud (CRM) (3.6 g of raw red mud), attaining a height in the column of 20 cm. A porous sheet was attached at the bottom of the column in order to support the adsorbent, and to ensure a uniform inlet flow and a good liquid distribution into the column. The top of the bed was closed with a 10 cm height layer of glass beads (1 mm diameter), which avoids the loss of material and also ensures a closely packed arrangement. A $200 \mu\text{g L}^{-1}$ As(V) solution was fed through the bed in up-flow mode at 5 mL min^{-1} using a peristaltic pump (Watson Marlow) connected at the bottom of the column. With this flow rate, an Empty Bed Contact Time (EBCT) of 28.27 minutes was attained. The pH of the incoming solution was maintained at 7. Samples were collected periodically using a homemade computer controlled fraction collector and As(V) concentration was determined as mentioned before.

3. Results and discussion

3.1. Raw materials characterization

Magnetite, Fe_3O_4 , was characterized in order to know the structure of this in-lab synthesized material. X-ray diffraction (XRD) analyses were developed on powdered samples of synthesized material. XRD pattern is shown in Figure 1, the position and relative intensity of all peaks match well with standard Fe_3O_4 powder diffraction data [17], indicating that the analysed sample is crystalline. It is important to note that, what

we are considering magnetite actually could be a mixture of magnetite and maghemite. Maghemite, $\gamma\text{-Fe}_2\text{O}_3$, being the fully oxidized counterpart of magnetite, can coexist with the latter because smaller Fe_3O_4 crystals are more easily transformed to $\gamma\text{-Fe}_2\text{O}_3$. However, it can also occur simultaneously with magnetite, the intermediate stages of magnetite oxidation result in nonstoichiometric oxides where magnetite actually seems to be partly oxidized [18]. It is generally a problem how to distinguish between nonstoichiometric magnetite and magnetite/maghemite mixtures because X-ray diffraction results are not conclusive in that respect. In many previous studies, iron oxide particles have been successfully synthesized through various methods and indexed to maghemite or magnetite based on the fact that its lattice parameter was closer to one of the both phases [19]. There are also studies where the distinction between magnetite and maghemite is done through comparison of their XRD patterns (peak position and intensities)[20]. In these studies, maghemite XRD pattern presented two peaks in the region $23 < 2\theta < 27$ which were not observed in our case in the magnetite pattern. As it can be seen in Figure 1, XRD pattern obtained for our in-lab synthesized product did not show the characteristic peaks assigned to the presence of maghemite. As stated before, X-ray diffraction results do not provide enough information, so more detailed characterization would be necessary to determine the exact structure of the synthesized iron oxide powder. Nevertheless, the aim of this work is the application of these materials as adsorbents; regardless of their composition, both magnetite and maghemite are iron oxides with similar structural, size and magnetic properties which make them potentially useful for As(V) removal.

SEM and TEM images were also obtained for in-lab synthesized magnetite. The pictures allow concluding that magnetite is formed by aggregates of nanoparticles. Figure 2 shows a representative example of the obtained SEM and TEM images.

Raw red mud was also characterized by XRD (data included as Supporting Information). Its spectra pattern indicates that red mud is a mixture of oxihydroxides but it does not allow distinguishing any distinctive crystalline phase. Red mud is a mixture of coarse sand and finer particles. Its composition, properties and phase vary with the type of the bauxite and the alumina production process. The main chemical composition of red mud is Fe_2O_3 , Al_2O_3 , SiO_2 , CaO , Na_2O , TiO , K_2O and MgO [21]. The broad distribution of different phases makes that XRD does not provide any useful information. Supporting Information also includes a particle distribution analysis of red mud, showing an extremely wide variety of particle diameter distribution of this heterogeneous material. Other characterization analysis of red mud and magnetite such as BET surface and FTIR spectra are also included in the Supporting information.

3.2. Effect of solution pH

pH is a key parameter in adsorption processes due to its influence on metal speciation and surface ionization. For this reason, adsorption experiments were carried out varying pH of the media, in order to determine the most favourable conditions for adsorption using raw materials.

As a waste of Bayer process, red mud is a solid that, in water solution, generates a very alkaline environment, with pH values around 10. Adsorption was evaluated under these basic conditions, as well as at lower pH values; results are collected in Figure 3. Good removal results were observed at pH below 7, achieving almost 100% of As(V) elimination. Nevertheless, at pH 10 no adsorption was observed. This fact can be explained taking into account the high hydroxyl concentration in solution that could inhibit the formation of complexes between As(V) anions and iron oxihydroxides. Considering these results, pH 7 was selected to develop further experiments with red

mud. This pH value allows achieving high removal percentages and, at the same time, reduces the amount of acid required to adjust the desired pH. In the case of magnetite experiments, no pH effect was observed in the range 2-7; removal percentages close to 100% were obtained in this broad pH range. These results are in good agreement with previous works [22, 23]. Thus, tests with magnetite were carried out at natural pH (≈ 5).

pH is a key factor in adsorption processes that affects both ionization and speciation of the substances present in solution, but it also affects to the surface charge of the sorbent material. Moreover, oxidation state and ionization are significant parameters that help understanding the interaction between contaminants and adsorbents. Eh-pH diagrams show that, in the pH range between 2 and 11, As (V) predominant forms are H_2AsO_4^- (at pH lower than 6.9) and HAsO_4^{2-} , both of them anionic species [1]. With respect to the ionization of the adsorbent surface, in the case of raw adsorbents, As(V) anions interact directly with the surface of the material. These materials, consisting of iron oxides, are positively or negatively charged depending on the pH. Zero charge potential pH (pH_{ZPC}) for iron oxides was found to be around 7 [22]; this means that the surface charge is positive below pH 7 and negative above it. Consequently the electrostatic interaction between the material surface and the arsenic anionic species is favourable for pH values below 7, achieving a 100% removal of arsenic as it can be seen in Figure 3.

Hybrid materials were not studied under various pH conditions. pH effect studied for raw materials indicates that As(V) removal is favourable at $\text{pH} \approx 7$, the natural pH obtained in the solution for hybrid materials, hence pH adjustment was not necessary.

3.3. Matrix selection

As it has been mentioned, the powdery nature of the sorbent materials selected in this study represents an important problem for separation after solution treatment as well as operational difficulties in continuous flow experiments. Consequently several immobilization matrixes were studied. Alginate, chitosan, silica and polyurethane foam were selected for matrix screening studies as a first step in the study of As(V) elimination. The raw materials tested demonstrated excellent removal capacities; attaining removal percentages close to 100% in all experiments as it can be seen in Figure 4. The experiment using magnetite was carried out at natural pH. However for red mud experiment the natural pH would raise close to 10, consequently the pH of the solution was adjusted to 6.5-7.

Silica gel [24-26] and polyurethane foam [27, 28] have been successfully use for immobilization in other studies, so they were tested in the present work. However, using these supporting materials arsenic elimination resulted completely inhibited and for this reason data were not included in Figure 4. Hence, despite these immobilization matrices were successfully tested in bibliography for other contaminants and sorbents, here they resulted to be inappropriate for As(V) removal.

On the contrary, good adsorption results were attained using chitosan and alginate as matrices, as it can be seen in Figure 4. Taking into account these results, chitosan and alginate blanks were performed in order to determine the adsorption capacity of the supporting material used in magnetite and red mud immobilization. These experiments, at pH 7, showed negligible arsenic adsorption in the concentration range tested. This fact indicates that the active material for arsenic removal in hybrid materials is not the supporting matrix. Such conclusion can be related with the structural composition of chitosan and alginate chains. Chitosan is a linear polysaccharide, which is composed by polymers of glucosamine and N-acetyl glucosamine. Most of the properties of chitosan

can be related to its cationic nature, its pKa depends on the deacetylation degree but in practice, it lies within 6.5-6.7 for fully neutralized amine functional groups [29]. On the other hand, alginates are polysaccharides consisting of 1→4 linked β-d-mannuronic acid and its C-5 epimer α-l-guluronic acid. Several studies have determined that pKa of alginate functions is around 3.5-4.6 [30, 31]. Both chitosan and alginate have pKa values lower than the pH used in the experimental conditions, which means that their active groups are mostly deprotonated. Therefore, electrostatic interaction with arsenate anions is not favourable. Figure 4 shows that chitosan immobilized materials are capable of retaining arsenic, maintaining high removal percentages. Hence, once immobilized, both red mud and magnetite keep up their capacity of retaining As(V). Since immobilization with alginate decreases red mud adsorption capacity, immobilization of magnetite with alginate was not tested.

Taking into account the screening results, only one immobilization method was proposed, using chitosan as supporting matrix, in order to improve mechanical characteristics of the selected materials for a subsequent application on larger scale maintaining good As(V) removal rates. Besides this, further adsorption experiments were carried out with raw materials with the aim of comparing their adsorption features before and after immobilization process.

Leaching batch tests were also performed with chitosan immobilized red mud. These experiments allowed proving that the metal release of hybrid material is negligible for all the metals tested (Al, As, Ba, Cd, Co, Cr, Cu, Fe, Mn, Mo, Ni, Pb, Sb, Se, Sn, Sr, Ti, Tl, V, Sn).

3.4.Kinetic studies

Kinetic studies were developed to determine the time necessary to attain the equilibrium in arsenic adsorption. These experiments were developed using both raw and immobilized materials.

First of all, equilibrium times were estimated using raw materials. In these studies As(V) concentration was fixed at 1 mg L^{-1} . Arsenic present in polluted waters is in the range of $\mu\text{g L}^{-1}$, and the maximum limits established by government agencies are lower than the selected value ($10 \mu\text{g L}^{-1}$ [3, 4]); however, 1 mg L^{-1} As(V) solutions were tested to ensure that equilibrium was attained using experimental conditions much more adverse than those found in arsenic polluted waters.

Both red mud and magnetite showed very fast As(V) removal. Equilibrium was almost instantaneous; in the first 5 min 80% of arsenic concentration was eliminated. In 10 min arsenic concentration in solution was negligible. Despite of the good removal results mentioned, these materials have some experimental drawbacks. As mentioned before, red mud solutions have a very high pH, which implies the need for adding large amounts of acid to maintain the optimum pH. Moreover, both red mud and magnetite have a powdery consistency, which implies that is very difficult to separate them from solution. In the case of magnetite, its magnetic nature makes easier its isolation in batch experiments by using a magnet. Nevertheless, their powdery nature hinders the application at large scale in both batch and column processes. For this reason the kinetics of immobilized materials has also been analysed.

Adsorption kinetics by hybrid materials, CM (chitosan coated magnetite) and CRM (chitosan coated red mud), were developed using the experimental conditions described above. Figure 5 shows the experimental data fitted using the pseudo second order model, which presents the following expression [32]:

$$q_t = \frac{q_e^2 kt}{1 + q_e \cdot kt} \quad (2)$$

where t represents the time in min, q_t is the adsorption at any time expressed in mg g^{-1} , q_e is the equilibrium adsorption (mg g^{-1}) and k is the rate constant ($\text{g mg}^{-1} \text{min}^{-1}$). A computer program was used to perform a non-linear fitting of time- q_t data using eq. 2. Table 1 summarizes the fitting parameters obtained with this model.

Equilibrium times were severely affected after the immobilization process. Before chitosan coating just a few minutes were enough to attain the equilibrium; on the contrary, after immobilization CM needs around 5 hours to attain equilibrium and CRM up to 15 hours. This behaviour could be expected taking into account that all immobilization processes imply the retard in the transport of the solute through the aqueous regions among the polymer chains; similar results were reported by Escudero and co-workers when comparing adsorption kinetics of raw and calcium alginate coated (hydr)oxide waste [33]. So the increase in the equilibrium time can be assigned to a worse diffusion. It is worth noting that the equilibrium times after chitosan immobilization are similar to other ones reported in bibliography for As(V) adsorbents [23, 33], therefore these materials maintain adsorption properties but they improve their mechanical characteristics.

In spite of the increase of equilibrium times, there are several advantages associated to the coating process. Once immobilized, red mud and magnetite do not form a suspension, the mechanical stability of the beads formed is more appropriate for high scale application and beads allow working in near-neutral pH solutions, so extreme pH values are avoided.

3.5. Equilibrium studies

Equilibrium studies were developed in order to determine the capacity of the materials employed for retaining As(V). The experiments were developed using both raw and immobilized materials, which allowed the comparison of their adsorption capacities. Taking into account that the data obtained did not approach an asymptote at high concentrations, experimental data were fitted to the Freundlich model in all cases. Freundlich isotherm is an empirical equation, which can be written as it follows:

$$q_e = K_f \cdot C_e^{1/n} \quad (3)$$

where K_f and n are Freundlich constants related to the strength of the sorbent-sorbate interaction and to the distribution of bond strengths among the surface sites of heterogeneous sorbents, respectively. The larger deviation of n from 1, the wider is the distribution of bond energies. As common for most soils, the condition $n > 1$ means that the bonding energies decrease with the increasing surface adsorption densities in concordance with preferential adsorption occupying surface sites in the order from strongest to weakest binding strength. Unlike the Langmuir equation, the Freundlich isotherm does not predict a maximum sorbate removal on the adsorption surface. This fact can be associated to the formation of a multilayer adsorption; in this case, the clearly defined maximum capacities envisioned by Langmuir isotherm may not occur.

The fitting values obtained for the Freundlich model are summarized in Table 2. As it can be seen, this model proved to be suitable to describe the experimental trend obtaining good regression coefficients for all fittings. Moreover, fitting parameter n was > 1 for all materials, which indicates multilayer adsorption where adsorption sites are occupied preferentially in order of their strongest binding strength.

Figure 6 shows the isotherms obtained for raw red mud and magnetite as well as the fitting curves corresponding to Freundlich model. Red mud is capable of adsorbing high

amounts of As(V), with adsorption capacities up to 100 mg g⁻¹. Magnetite also shows very good properties as As(V) adsorbent, although its arsenic removal capacity is less effective than that of red mud.

It is interesting to compare the adsorption capacities obtained before and after immobilization; the modification in the behaviour of immobilized materials is also reflected in Figure 6. As it can be seen in this figure, immobilization process obstructs the adsorption capacity of red mud to adsorb As(V); this fact can be associated to the decrease in the accessibility to the active surface of red mud after the immobilization with chitosan. Once immobilized the active sites of red mud are less accessible, which explains both the decrease in adsorption capacity and the increase in adsorption time necessary to attain the equilibrium, as mentioned before. Moreover, immobilization process can also proceed through the reaction of binding sites with the coating agent and thus reducing the adsorption capacity of red mud.

The case of magnetite shows that the observed behaviour is just the opposite; it can be seen that immobilized magnetite has better adsorption capacity than that of the raw material. This fact could be assigned to the immobilization process followed. During this process, the magnetite was dissolved in the coating agent using ultrasound agitation; the sonication may facilitate the dispersion of the aggregated magnetite nanoparticles. Once dispersed, magnetite particles have a larger surface area than the starting raw material, where the magnetite was formed by aggregates. The increase in the specific area would make that immobilized magnetite presented higher adsorption capacity than raw magnetite. This hypothesis was confirmed by developing several experiments (varying initial As(V) concentration) where raw magnetite was previously dispersed by ultrasonic agitation. These experiments showed that dispersed magnetite had better adsorption capacities than non-dispersed material, achieving an increase in the

adsorption capacity of approximately 30% for low concentrations (initial concentration $<400 \text{ mg L}^{-1}$) and around 25% when the initial concentration was higher than 600 mg L^{-1} (see Figure 6). These results allowed confirming that ultrasonic dispersion affects the adsorption capacity of raw magnetite. Comparing these results with those obtained for CM they resulted to be quite similar, which means that immobilization processes did not affect the adsorption capacity once raw magnetite was previously dispersed by sonication.

Finally, Figure 6 also allows comparing adsorption isotherms for both immobilized materials. After coating, adsorption capacities of red mud and magnetite become comparable, maintaining excellent adsorption capacities.

Maximum sorption capacities for other materials tested by other authors are collected in Table S1 of the Supporting Information. Although our isotherms data did not achieve saturation values, the highest values observed with our materials (as high as 100 mg g^{-1}) are among the highest values found for other materials tested in As(V) removal.

3.6. Column experiments

One of the main topics of debate in wastewater treatment is that of batch processing versus continuous flow. Batch process presents some advantages like flexibility when the feed water quality changes, easy cleaning, simple automatic controls or low investment cost. On the other hand, it is widely recognized that a fixed-bed sorption process is operationally simple, requires virtually no start-up time and avoids fluctuations in feed composition. In this work all experiments indicated that immobilized red mud and magnetite present good adsorption properties in batch mode, but it is also interesting to study the behaviour of these materials under continuous flow. This is the reason why column experiments were developed as a first approach to the

application of the adsorbents studied in the industrial/natural wastewater treatment. Taking into account batch experiments, CRM was selected as the best candidate to a high scale application. Immobilization process allowed solving experimental problems related to the high solution pH values or the small particle size associated to the use of raw red mud, maintaining high adsorption capacities and moderate equilibrium times. Raw red mud tends to raise the pH of the solution above 10, making necessary the addition of large amounts of acid to compensate this undesirable pH value. Besides, its powdery nature makes red mud prone to clog any small size retention mesh located at the exit of the column meanwhile a large size retention mesh will be totally ineffective for material retention in the column. Moreover, red mud is considered as a residue and hence it is a cost-effective material. Magnetite was discarded in this continuous flow study because its time-consuming synthesis makes difficult to obtain the large amount of material required for filling the column. The price to prepare such a large amount of magnetite would also be another drawback to take into consideration.

Taking into account the high adsorption capacity of immobilized red mud observed in isotherm studies, a concentrated solution of As(V) was tested in the column experiment. Figure 7 represents the breakthrough curve obtained. As it can be seen, the column was operating during more than 10 days before the inlet As(V) concentration was attained at the exit. This figure also shows how the breakthrough curve has two different regions; at short times the curve has a sharp slope, corresponding with the first 24 hours. After this time, the slope becomes less steep until the curve reaches the inlet concentration of $200 \mu\text{g L}^{-1}$. This could be related with the contribution of different kind of active sites in these two regions. Although a simple two parameter model have been proposed to describe column profiles [34, 35], in hour case, since the column does not show the typical sigmoid shape, this model can not be applied. Numerical integration of the

column profile allows calculating the amount of arsenic retained in the column, which was 4.44 mg, so 1.23 mg per gram of red mud or 0.222 mg per gram of hybrid material. Column test allowed confirming that, once saturated, CRM maintain its excellent physical and mechanical properties; which makes it a promising hybrid material with optimal characteristics to apply in hydrodynamic processes. The breakthrough curve obtained also showed that As(V) is present in the outlet since the beginning of the operation, which indicates that column process is not the best alternative for treating highly concentrated As(V) solutions. Therefore, for high As concentrations, batch process may be the best option for better arsenic removal results.

4. Conclusions

This study allowed comparing adsorption capacities of different geomaterials. Experimental results bore out the excellent capacity of iron oxihydroxides based materials to retain As(V) from solution. Further analysis concerning red mud and magnetite demonstrated the high efficiency of these materials in As(V) removal. Synthetic nanostructured magnetite was found as a pH-independent adsorbent, achieving high removal percentages in few minutes. On the other hand, red mud (a residual by-product of Bayer process) resulted in a better As(V) adsorbent than synthetic magnetite after an appropriate pH adjustment. At pH 7 red mud was capable of achieving legal standards for drinking water ($<10 \mu\text{g L}^{-1}$) from an As(V) polluted water.

Immobilization process was studied using several matrixes. Chitosan coated materials showed the best results; hence this was the selected material for red mud and magnetite coating. Practical drawbacks of raw materials such as small particle size or high basicity were solved by chitosan coating; maintaining high adsorption capacities and moderate equilibrium times. Finally, batch application was selected as the best option for large-

scale wastewater treatment considering the results obtained in continuous flow experiment.

5. Acknowledgements

Authors wish to thank Ministerio de Economía y Competitividad for the financial support through the research Project CTM2012-37272, cofounded with FEDER programme.

References

- [1] D. Mohan, C.U. Pittman Jr., Arsenic removal from water/wastewater using adsorbents-A critical review, *J. Hazard. Mater.* 142 (2007) 1-53.
- [2] World Health Organization, Arsenic in drinking-water: background for development of WHO guidelines for drinking-water quality, (2011).
- [3] European Commission, COUNCIL DIRECTIVE 98/83/EC of 3 November 1998 on the quality of water intended for human consumption, *Official Journal of the European Union*, 1998.
- [4] United States Environmental Protection Agency, National primary drinking water regulation; Arsenic and clarifications to the compliance and new source contaminants monitoring, *Daily Journal of the United States Government* 66 (2001) 6976-7066.
- [5] H. Genç-Fuhrman, J.C. Tjell, D. McConchie, Adsorption of Arsenic from Water Using Activated Neutralized Red Mud, *Environmental Science & Technology* 38 (2004) 2428-2434.
- [6] V.M. Boddu, K. Abburi, J.L. Talbott, E.D. Smith, R. Haasch, Removal of arsenic (III) and arsenic (V) from aqueous medium using chitosan-coated biosorbent, *Water Res.* 42 (2008) 633-642.

- [7] M. Martínez-Cabanas, L. Carro, M. López-García, R. Herrero, J.L. Barriada, M.E. Sastre de Vicente, Achieving sub-10 ppb arsenic levels with iron based biomass-silica gel composites, *Chem. Eng. J.* 279 (2015) 1-8.
- [8] P. Lodeiro, S.M. Kwan, J.T. Perez, L.F. Gonzalez, C. Gerente, Y. Andres, G. McKay, Novel Fe loaded activated carbons with tailored properties for As(V) removal: Adsorption study correlated with carbon surface chemistry, *Chem. Eng. J.* 215 (2013) 105-112.
- [9] E. Guibal, Interactions of metal ions with chitosan-based sorbents: a review, *Sep. Purif. Technol.* 38 (2004) 43-74.
- [10] M. Rinaudo, Chitin and chitosan: Properties and applications, *Prog. Polym. Sci.* 31 (2006) 603-632.
- [11] L. Pontoni, M. Fabbricino, Use of chitosan and chitosan-derivatives to remove arsenic from aqueous solutions - a mini review, *Carbohydr. Res.* 356 (2012) 86-92.
- [12] P. Miretzky, A.F. Cirelli, Hg(II) removal from water by chitosan and chitosan derivatives: A review, *J. Hazard. Mater.* 167 (2009) 10-23.
- [13] R.H. Wijffels, *Immobilized cells*, Springer-Verlag, Berlin ; New York, 2001.
- [14] M. Yamaura, D. Alves Fungaro, Synthesis and characterization of magnetic adsorbent prepared by magnetite nanoparticles and zeolite from coal fly ash, *J Mater Sci* 48 (2013) 5093-5101.
- [15] T. Coradin, M. Amoura, C. Roux, J. Livage, M.C. Flickinger, *Biocers, Industrial Applications*, Encyclopedia of Industrial Biotechnology, John Wiley & Sons, Inc.2009.
- [16] J. Moreda-Piñeiro, C. Moscoso-Pérez, P. López-Mahía, S. Muniategui-Lorenzo, E. Fernández-Fernández, D. Prada-Rodríguez, Multivariate optimisation of hydride generation procedures for single element determinations of As, Cd, Sb and Se in natural waters by electrothermal atomic absorption spectrometry, *Talanta* 53 (2001) 871-883.

- [17] W. Kim, C.-Y. Suh, S.-W. Cho, K.-M. Roh, H. Kwon, K. Song, I.-J. Shon, A new method for the identification and quantification of magnetite–maghemite mixture using conventional X-ray diffraction technique, *Talanta* 94 (2012) 348-352.
- [18] R.E. Vandenberghe, C.A. Barrero, G.M. da Costa, E. Van San, E. De Grave, Mössbauer characterization of iron oxides and (oxy)hydroxides: the present state of the art, *Hyperfine Interact.* 126 (2000) 247-259.
- [19] F.-Y. Cheng, C.-H. Su, Y.-S. Yang, C.-S. Yeh, C.-Y. Tsai, C.-L. Wu, M.-T. Wu, D.-B. Shieh, Characterization of aqueous dispersions of Fe_3O_4 nanoparticles and their biomedical applications, *Biomaterials* 26 (2005) 729-738.
- [20] D. Maity, D.C. Agrawal, Synthesis of iron oxide nanoparticles under oxidizing environment and their stabilization in aqueous and non-aqueous media, *J. Magn. Magn. Mater.* 308 (2007) 46-55.
- [21] P. Wang, D.-Y. Liu, Physical and Chemical Properties of Sintering Red Mud and Bayer Red Mud and the Implications for Beneficial Utilization, *Materials* 5 (2012) 1800-1810.
- [22] J. Giménez, M. Martínez, J. de Pablo, M. Rovira, L. Duro, Arsenic sorption onto natural hematite, magnetite, and goethite, *J. Hazard. Mater.* 141 (2007) 575-580.
- [23] H. Basu, R.K. Singhal, M.V. Pimple, A.V.R. Reddy, Arsenic Removal from Groundwater by Goethite Impregnated Calcium Alginate Beads, *Water, Air, & Soil Pollution* 226 (2015) 1-11.
- [24] L. Carro, E. Hablot, T. Coradin, Hybrids and biohybrids as green materials for a blue planet, *J. Sol-Gel Sci. Technol.* 70 (2014) 263-271.
- [25] C. Depagne, C. Roux, T. Coradin, How to design cell-based biosensors using the sol–gel process, *Analytical and Bioanalytical Chemistry* 400 (2011) 965-976.

- [26] S. Ramachandran, T. Coradin, P. Jain, S. Verma, *Nostoc calcicola* Immobilized in Silica-coated Calcium Alginate and Silica Gel for Applications in Heavy Metal Biosorption, *Silicon* 1 (2009) 215-223.
- [27] M. Valodkar, P.S. Rathore, P. Sharma, D. Kanchan, M. Patel, S. Thakore, Immobilization of metal nanoparticles on polyurethane membranes: synthesis and electrical properties, *Polym. Int.* 61 (2012) 1745-1750.
- [28] D.M. Carrero, J.M. Morales, A.C. Garcia, N. Florez, P.A. Delgado, J. Dussan, A.C. Uribe, A.F.G. Barrios, Comparative analysis for three different immobilisation strategies in the hexavalent chromium biosorption process using *Bacillus sphaericus* S-layer, *The Canadian Journal of Chemical Engineering* 89 (2011) 1281-1287.
- [29] G. Crini, P.-M. Badot, Application of chitosan, a natural aminopolysaccharide, for dye removal from aqueous solutions by adsorption processes using batch studies: A review of recent literature, *Prog. Polym. Sci.* 33 (2008) 399-447.
- [30] C. De Stefano, A. Gianguzza, D. Piazzese, S. Sammartano, Modelling of proton and metal exchange in the alginate biopolymer, *Analytical and Bioanalytical Chemistry* 383 (2005) 587-596.
- [31] C. Rey-Castro, R. Herrero, M.E. Sastre de Vicente, Gibbs-Donnan and specific ion interaction theory descriptions of the effect of ionic strength on proton dissociation of alginic acid, *J. Electroanal. Chem.* 564 (2004) 223-230.
- [32] S. Azizian, Kinetic models of sorption: a theoretical analysis, *J. Colloid Interface Sci.* 276 (2004) 47-52.
- [33] C. Escudero, N. Fiol, I. Villaescusa, J.-C. Bollinger, Arsenic removal by a waste metal (hydr)oxide entrapped into calcium alginate beads, *J. Hazard. Mater.* 164 (2009) 533-541.

[34] A. Chatterjee, S. Schiewer, Multi-resistance kinetic models for biosorption of Cd by raw and immobilized citrus peels in batch and packed-bed columns, Chem. Eng. J. 244 (2014) 105-116.

[35] A. Chatterjee, S. Schiewer, Effect of Competing Cations (Pb, Cd, Zn, and Ca) in Fixed-Bed Column Biosorption and Desorption from Citrus Peels, Water Air and Soil Pollution 225 (2014).

Tables

Table 1.- Pseudo-second order parameters obtained from experimental data fittings. Highest sorption capacities measured: CRM 0.31 mg g⁻¹(after 23 hours of contact time), CM 0.33 mg g⁻¹ (after 8.5 hours contact time).

| Material | r ² | q _e /mg·g ⁻¹ | k/g·mg ⁻¹ ·min ⁻¹ |
|----------|----------------|------------------------------------|---|
| CRM | 0.977 | 0.31±0.01 | 0.08±0.01 |
| CM | 0.998 | 0.343±0.002 | 0.243±0.009 |

Table 2.- Freundlich fitting parameters for the materials studied

| Material | r ² | K _f | n |
|-----------|----------------|----------------|-----------|
| Red Mud | 0.979 | 1.16±0.37 | 1.28±0.10 |
| CRM | 0.943 | 0.26±0.18 | 1.15±0.15 |
| Magnetite | 0.988 | 0.43±0.11 | 1.35±0.07 |
| CM | 0.996 | 0.4±0.1 | 1.23±0.05 |

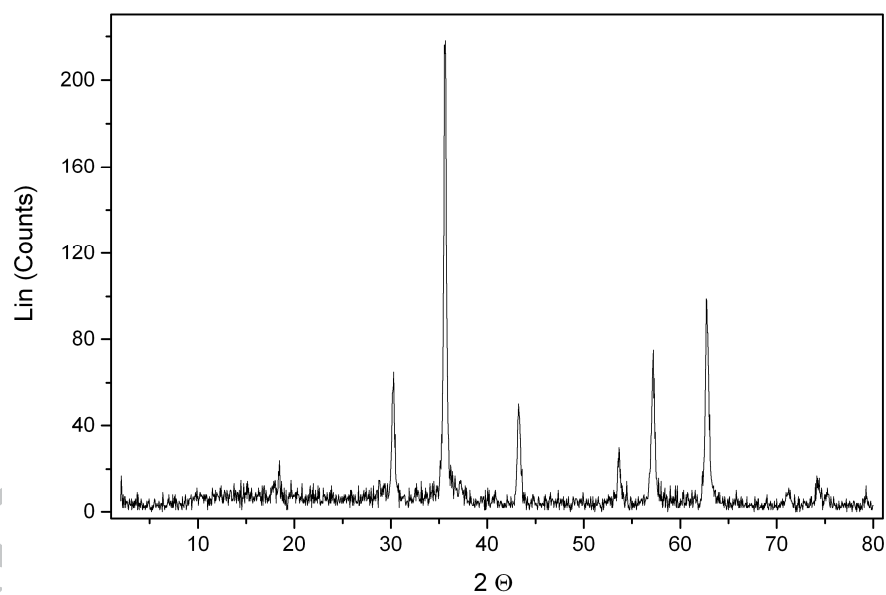
Figures**Figure 1.-** XRD pattern of magnetite (Fe_3O_4)

Figure 2.- SEM (a) and TEM (b) images obtained for in-lab synthesized magnetite.

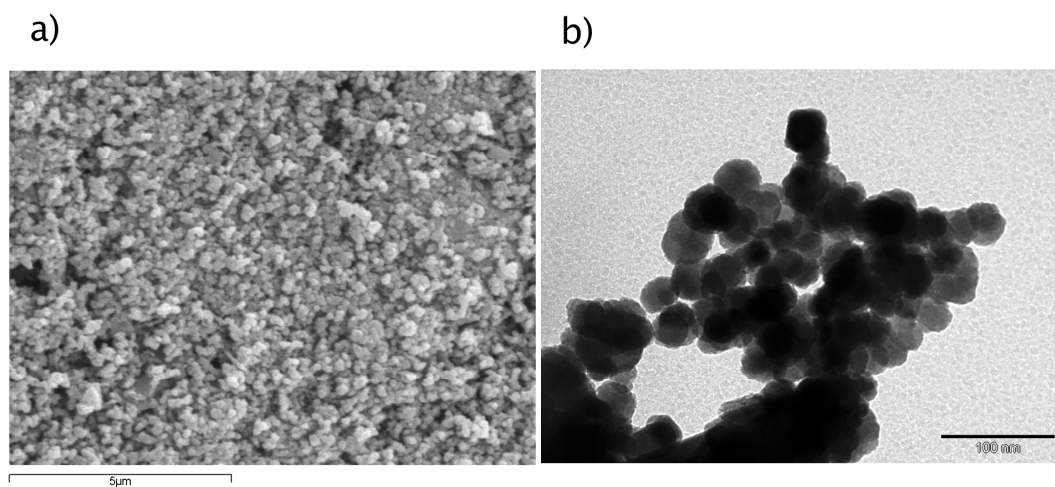


Figure 3.- Effect of solution pH on As(V) adsorption using red mud (red circles) and magnetite (grey squares). As(V) initial concentration $50 \mu\text{g L}^{-1}$.

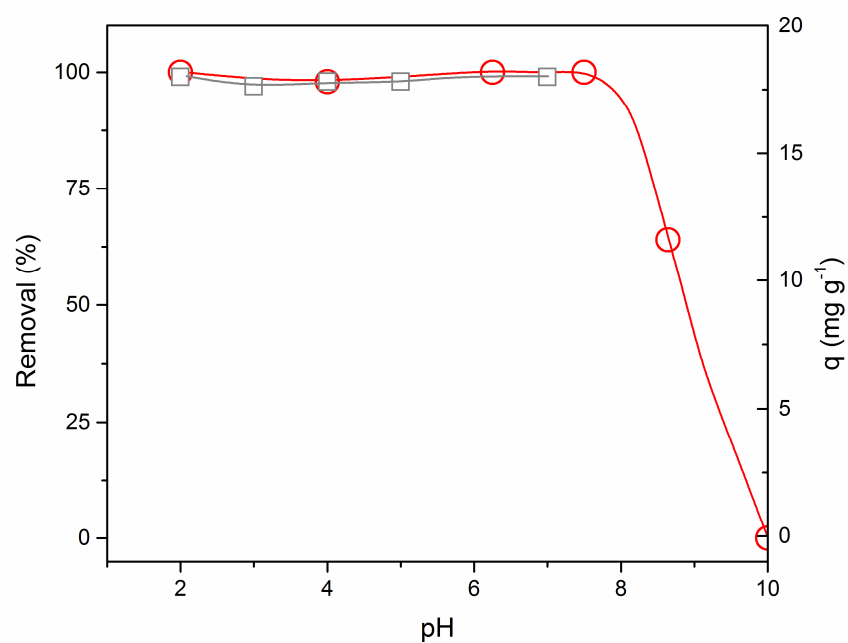


Figure 4.- Removal percentages for arsenic. Material dose 2.5 g L^{-1} . Initial concentration $50 \text{ } \mu\text{g L}^{-1}$. No pH modification, natural pH close to 7, except for red mud, where pH was adjusted to 7. Contact time 24 h at $25 \text{ }^{\circ}\text{C}$.

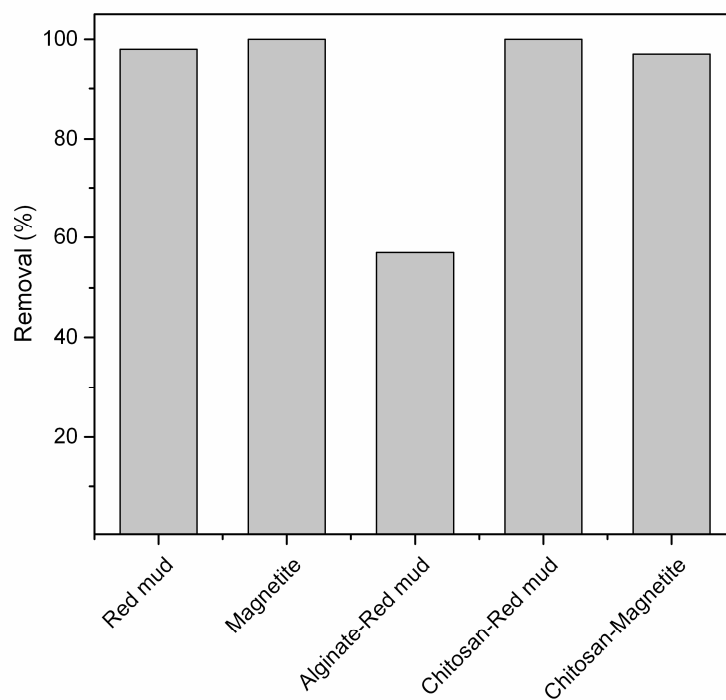


Figure 5.- Kinetics of CRM (grey circles) and CM (grey squares) fitted to the pseudo second order model (solid lines). Material dose 2.5 g L^{-1} , As(V) initial concentration 1 mg L^{-1} , pH 7 at 25°C . Open symbols correspond to the kinetic study done with raw materials.

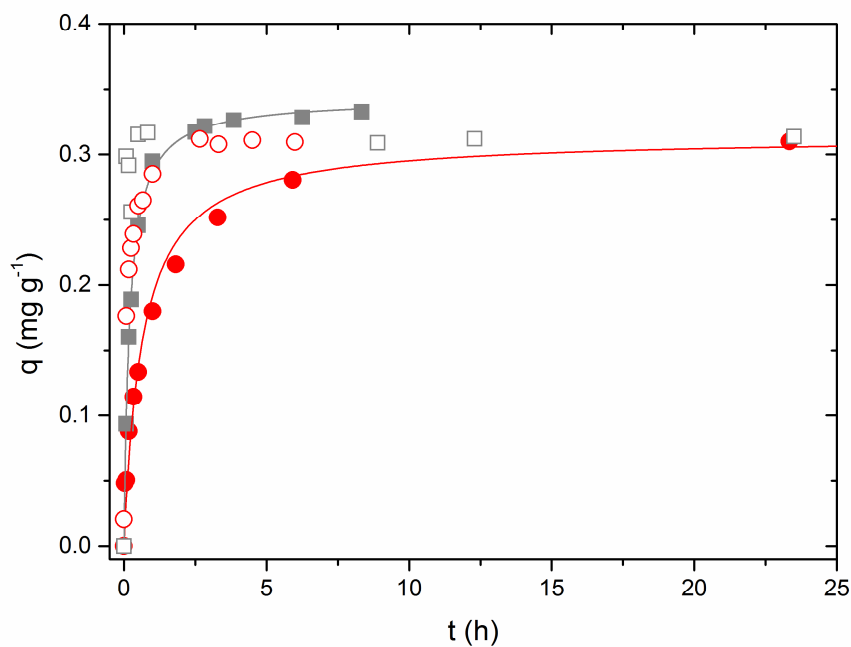


Figure 6.- Isotherms for magnetite (squares) and red mud (circles). Solid symbols correspond to chitosan immobilized materials and open symbols represent raw materials. Solid and dotted lines represent the Freundlich fitting. Adsorbent dose 2.5 g L^{-1} , pH 7. Triangles correspond to the experiments done with raw magnetite, dispersed with sonication.

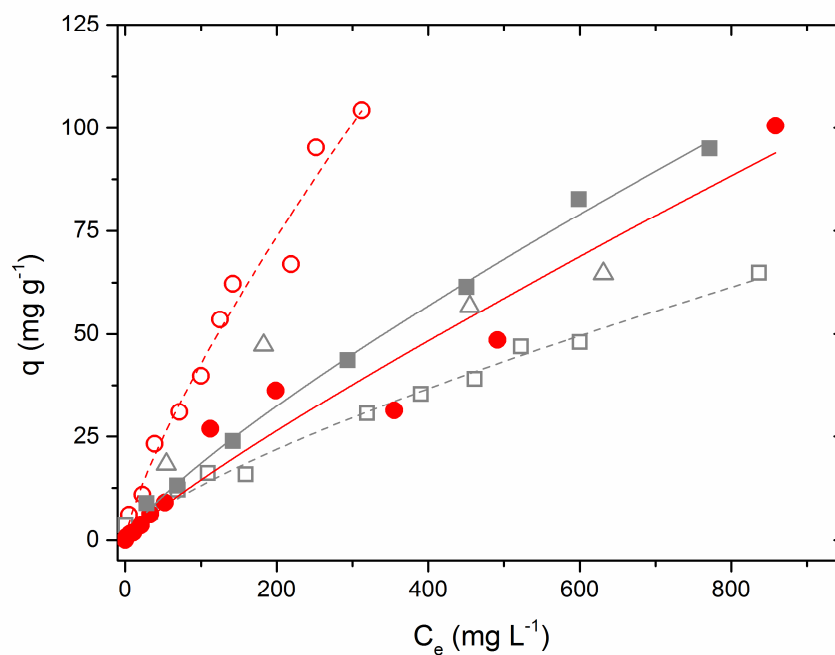
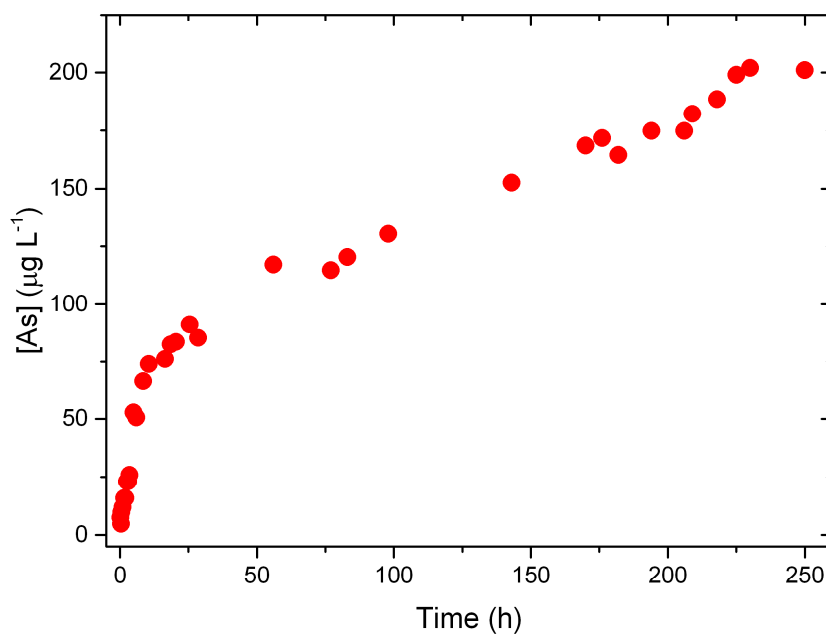


Figure 7.- Continuous experiment for As(V) removal. As(V) initial concentration 200 $\mu\text{g L}^{-1}$, red mud dose 3.60 g, pH 7. Bed height 20cm and flow rate 5 mL min^{-1} .



Highlights

- Chitosan constitutes a good polymer for iron oxide immobilization
- Sorption properties of iron oxides are not inhibited by chitosan coating
- Hybrid materials present good mechanical properties for water pollution treatment
- Arsenic can be efficiently removed using cost-effective hybrid polymeric materials

ACCEPTED MANUSCRIPT